

Full Length Research Paper

Recent uranium mobilization and radioactivity of metamorphosed sandstones at Sikait area, South Eastern desert of Egypt

Soliman A. Abu Elatta¹, S. F. Hassan¹, A. H. El-Farrash², M. G. El-Feky^{1*} and M. Refaat¹

¹Nuclear Material Authority, El-maadi, Cairo, Egypt.

²Physics Department, Faculty of Science, Mansoura University, Mansoura, Egypt.

Received 24 February, 2014; Accepted 25 March, 2014

The metamorphosed sandstones exposures occur in two locations in Wadi Sikait. The exposed rocks in this area are ophiolitic mélangé, metamorphosed sandstones, porphyritic granites invaded by post-granite dykes (lamprophyres) and quartz-fluorite veins. The uranium contents measured radiometrically range from 3 to 41.97 ppm, with an average of 12 ppm, while the chemically measured are in the range from 20 to 100 ppm and averaging 50.83 ppm. High uranium contents are mainly attributed to the presence of secondary uranium minerals (uranophane and autonite), accessory minerals (monazite, zircon, allanite and xenotime) and U-bearing minerals (muscovite, biotite, chlorite, iron oxides and clays). P- and D-factors indicate disequilibrium in U-decay due to addition of uranium in these rocks. Since radioactive secular equilibrium of the young age deposits have not yet reached, therefore, the activity ratios (AR) of $^{230}\text{Th}/^{234}\text{U}$ in the studied rocks is very small and ranges from 0.43 to 1.3. Radon exhalation rates of the studied rocks were also measured using “Sealed Can technique” and indicated the presence of subsurface and surface uranium anomaly which confirms the previous results.

Key words: Metamorphosed sandstones, uranium, minerals, Wadi Sikait.

INTRODUCTION

The natural environmental radiation depends mainly on geological and geographical conditions (Florou and Kritidis, 1992). Higher radiation levels are associated with igneous rocks, such as granite and lower levels with sedimentary rocks. There are exceptions, however, as some shales and phosphate rocks have relatively high content of radionuclides (UNSCEAR, 1993). The study area lies in the southern part of the Eastern Desert of

Egypt along the upper stream of Wadi Sikait (Figure 1).

Wadi Sikait area is covered by moderate to high mountains with rugged topography. The high peak is Gabal Sikait (769 m a.s.l); it is formed of ultramafic rocks, which are often associated with beryl mineralization. The Sikait area was geologically investigated by Hashad and El Redy (1979), Hegazy (1984), Hassan and Hashad (1990), Omar (1995), Mohamed and Hassanen (1997),

*Corresponding author. E-mail: mglal_99@hotmail.com

Author(s) agree that this article remain permanently open access under the terms of the [Creative Commons Attribution License 4.0 International License](https://creativecommons.org/licenses/by/4.0/)



Figure 1. Aerial photograph showing Location of the studied areas.

Saleh (1998), Ibrahim et al. (1999) and Saleh et al. (2012), among others.

The Wadi Sikait area, in the south Eastern Desert of Egypt is located along the low-angle thrust zone of the Nugrus Thrust Fault (El-Ramly et al., 1984) and may represent a zone of discontinuity between two domains, the central and southern parts of the Eastern Desert (Stern and Hedge, 1985). This thrust fault separates the medium metamorphic grade associations, dominantly metapelites and gneiss, from the lower metamorphic grade ophiolitic melange assemblage, with subordinate metasediments in its footwall (Greiling et al., 1988; Harraz and EL-Sharkawy, 2001; Saleh et al., 2012). The region is composed of metapelitic schists, gneisses and granites and is cut by a number of dykes of different compositions, together with various types of aplitic and pegmatitic veins. Greiling et al. (1994) concluded that post collisional evolution in Eastern Desert of Egypt started with extensional collapse, which was followed by NNW-SSE shortening and related large - scale thrusting (toward the NNW) and folding, distributed all over the Eastern Desert, followed by further period of Late to Post-activity.

Assaf et al. (2000) studied the polyphase folding in Nugrus-Sikait area and reported that the lithological constitution of the area comprise a sequence of dismembered ophiolites, ophiolitic mélangé association and arc assemblage. The older rocks are intensively deformed and intruded by intracratonic association, which, within the mapped area, is ophiolitic mélangé, metamorphosed sandstones with porphyritic granites. Planer and linear mesoscopic structures exhibited by the rocks of the area indicate that these rocks are involved in

superimposed folding events and at least three folding generations.

Detailed spectrometric radiometric study (Ibrahim et al., 2007) for metamorphosed sandstones site at Wadi Sikait indicate that eU range from (15 to 100 ppm), but chemically range from (60 to 480 ppm); whereas eTh was up to 85 ppm. Also, they reported that the emplacement of both lamprophyre dykes and porphyritic granites may play important role as a heat source, which lead to U-mobilization from hot granitic magma, transported (along deep fault and banding) and redeposited in metamorphosed sandstones under suitable conditions. The present work aims to study the radioactivity of Sikait metamorphosed sandstone and clarify the evidences of recent U-mineralization of these rocks.

METHODOLOGY

Analytical techniques

A variety of samples, comprising various degrees of alteration were investigated using the following five techniques: (1) Petrographic study, (2) autoradiographic analysis, (3) environmental scanning electron microscope examination, (4) NaI(Tl) and HPGe-detectors, and (5) uranium chemical analysis. An autoradiographic investigation was carried out for studying the forms of the radioactive mineralizations in the studied samples. Alpha-sensitive cellulose-nitrate film was sandwiched between the thin-polished section and a glass slide. Exposure time varied from 21 to 30 days. Calibration of NaI(Tl) detector was carried out by using Co-57 gamma source (122.1 KeV, set up in channel 122) and Cs-137 source (661.6 KeV, set up in channel 662). The unknown samples were measured through the system and then related to the standard sources of U, Th, Ra and K, provided by the International Atomic Energy Agency (IAEA). A computer program analysis,

written in Pascal language (Matoline, 1991) and run under MS-Dos, has been used to calculate the concentrations of (U, Th and Ra in ppm) and K (in %).

Geological setting

The field mapping indicates that metamorphosed sandstones occur in two sites at Wadi Sikait (Sikait-1 and Sikait-2) (Figure 1) and the exposed rocks at this area can be arranged based on field observations and structural relations from older to younger as follows:

1. Veins (fluorite and quartz) youngest;
2. Lamprophyre dykes;
3. Porphyritic granites;
4. Metamorphosed sandstones;
5. Ophiolitic mélange oldest.

Ophiolitic mélange

The ophiolitic mélange in the study area occurs on the Eastern side of Wadi Sikait. It is composed of ophiolitic block rocks (mafic and ultramafic) tectonically embedded in highly pervasively deformed matrix of metasedimentary origin and rock fragments of meta-peridotite, meta-pyroxenite and meta-gabbros, different in sizes and shapes. The metasedimentary matrix is highly folded and sheared schists (quartzo-feldspathic schist, garnet micaschist, tourmaline-garnetiferous schist, graphite schist, sillimanite schist and talc schist). Also, many microstructures were found in the matrix as foliations, boudins, mineral lineations and minor folding. The most foliation planes are parallel to the plane of Nugrus thrust. The ophiolitic blocks represented about 2% of the total ophiolitic mélange and are characterized by highly serpentinized or transformed into talc-carbonate in many places with creamy color.

Metamorphosed sandstones

The metamorphosed sandstones occur in two locations in Wadi Sikait. The first location (Sikait-1) lies at the upper stream of Wadi Sikait and the second location (Sikait-2) occurs west the bend of Wadi Sikait (Figure 2a and b). The metamorphosed sandstone rocks are fine- to medium- grained, white color, highly sheared, sometimes bedded, cross-cut by lamprophyre dykes (NW-SE and NNE-SSW), quartz veins and left strike slip faults (NW-SE, NNE-SSW and N-S) (Figure 3a). Sikait-1 is the largest outcrop of metamorphosed sandstones at Wadi Sikait, with low to medium peaks, elongated in NW-SE direction (1.4 km in length and range in width from 120 to 300 m) (Figure 3b). These rocks range in color from pale white to milky white (Figure 3c) and show relics of primary bedding; banding and obvious foliations in NW-SE with angle of dip 35°/SW (Figure 3d). Metamorphosed sandstones in this location are dissected by three types of left strike slip faults, N-S and NNE-SSW and NW-SE (Figure 3e), so that they are highly tectonized. The NW-SE is the largest and oldest one. These faults, especially NNE-SSW, are characterized by mylonitization and many types of alterations as silicification and Fe-Mn oxy-hydroxides (Figure 3f). Mineralization occurs along zones of these faults visible to the naked eyes.

Sikait-2 covers a small area where its length is about 450 m and maximum width about 230 m, forming low terrain, highly sheared, dissected by branches of strike slip fault running in N-S with left movements and frequently curved to N direction. Branch zones of

the strike slip fault characterized silicification alteration. Many mineralizations are associated with quartz found along zones of fault branches as fluorite at west of this location and wolframite and cassiterite which are visible to naked eyes. Metamorphosed sandstones are generally uniform in texture and composed of fused quartz grains. Semi-angular and elongated rock fragments of older rocks are enclosed in metamorphosed sandstones.

Microscopically, the metamorphosed sandstones at this location are fine- to medium grained, with whitish grey color and vary in composition from greywacke to arkose. The secondary uranium minerals in these rocks at Sikait-1 are filling pore spaces between crystals, associated with the strike slip faults (especially NNE-SSW and NW-SE), or in both broken and surfaces of crystals near these faults (Figure 4a to d).

Greywacke is composed essentially of quartz, sodic plagioclase, K-feldspars and biotite as well as garnet and fluorite, zircon and allanite as accessories while chlorite and sericite (muscovite) is the alteration products. Quartz (66% in vol.) occur in two generations; the first one is euhedral shape, showing undulated extension and corroded in plagioclase while the second is squeezed among primary minerals and filling fractured plagioclase and may be formed related to the structured affected in the area. Plagioclase (An₇₋₁₂) is characterized by a representation of 32% in vol. of the rock, subhedral to anhedral crystals, highly deformed twinning and partially sericitized. K- Feldspars are represented by microcline, orthoclase and orthoclase micropertite phenocrysts. The longest axes of these crystals are parallel to the strike of foliation. K- Feldspars is subjected to the different degrees of kaolinitization. Biotite crystals occur as subhedral flakes and most of them showed foliations, partially altered to chlorite along their cleavages, showing foliations (Figure 4e). Sometimes biotite is distributed through the rock and/or sometimes segregated in folded layer. Muscovite occurs as aggregates associated with biotite or plagioclase. Zircon occurs as euhedral to subhedral prismatic crystals and some of them are metamict (Figure 4f). Allanite occurs as subhedral to anhedral crystals with among the same primary minerals. Fluorite occurs as considerable amount, filling the space among primary minerals or as inclusions in plagioclase. Garnet occurs as subhedral crystals.

Arkoses are composed essentially of quartz and feldspars as well as opaques, zircon and allanite while sericite is the main alteration product. Quartz (80% in vol.) occurs as polygonal shape and sometimes showed undulated extension as a result of the strain affected. Feldspars (18% in vol.) are represented by albite (14% in vol.) and perthite (4% in vol.). Albite occurs as subhedral to anhedral crystals, taking preferred orientation. Most of these crystals are cracked and corroded by/or contains quartz. Perthite crystals occur as anhedral cracked string type. Opaques are rare and occur as skeletal shape; zircon occurs as short prisms terminated by two pyramids. Allanite occurs as subhedral to anhedral crystals among the primary minerals.

Porphyritic biotite granite

Porphyritic biotite granite is characterized by grey to whitish pink color, coarse to very coarse-grained, with k-feldspars crystals up to 2 cm and composed mainly of quartz, plagioclase, k-feldspars and biotite. This rock is marked with sharp contacts with metamorphosed sandstones and contains xenoliths of it. Most k-feldspars crystals take preferred orientation parallel to the general direction of the biotite flakes. Porphyritic biotite granite cuts by both lamprophyre dykes and strike slip faults occur in study area. Strike slip faults are characterized by reddish color along fault zones, brecciate, gouge structure and barren quartz vein sometimes. Porphyritic biotite granite is mylonitized at the east side of the Sikait-2 due to affected major faults.

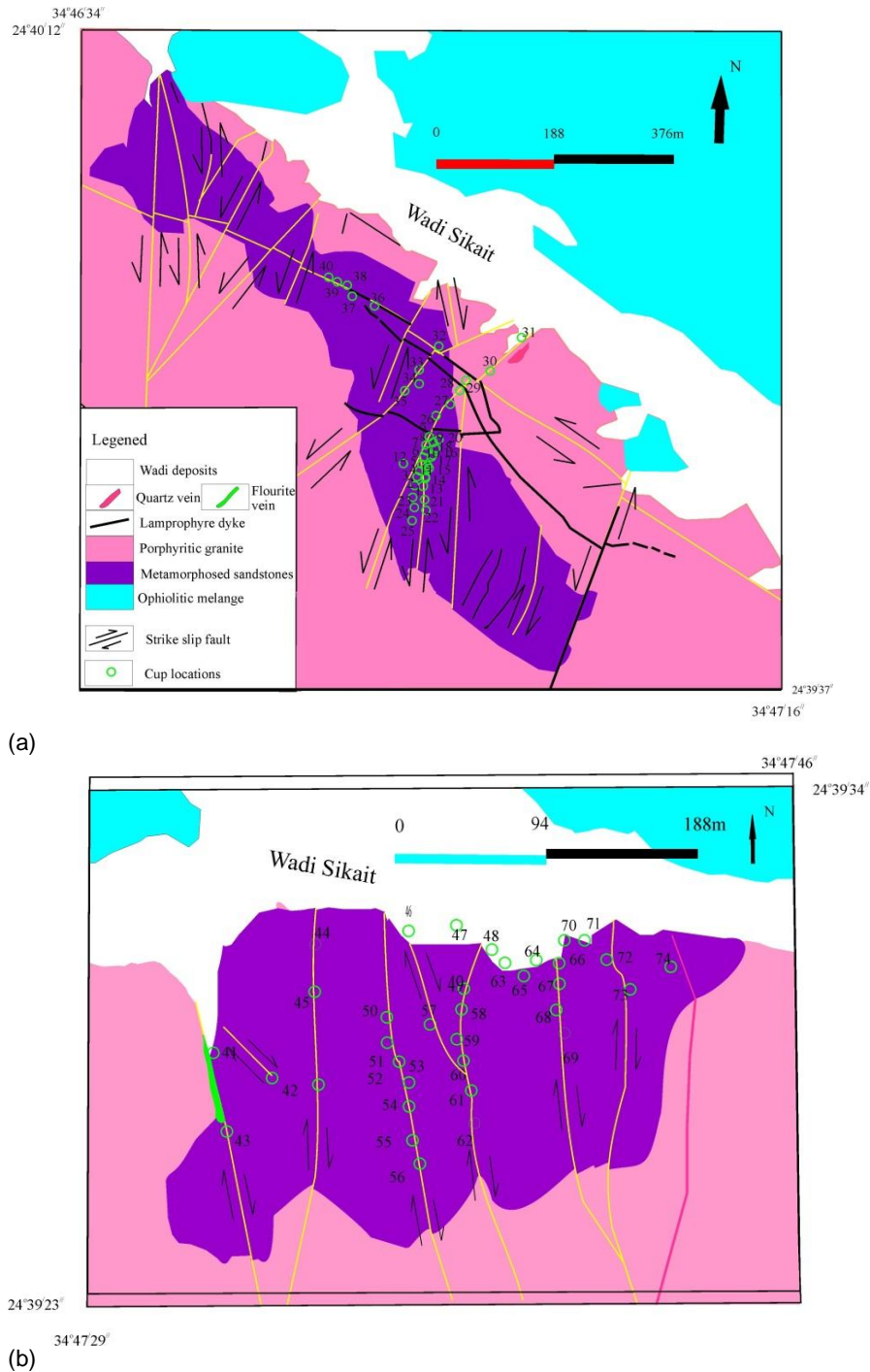


Figure 2. Detailed geologic map of Sikait-1(a) and Sikait-2 (b) (Ibrahim et al., 2010).

Lamprophyre dykes

Lamprophyre dykes are compact, black or dark black in color, altered, fine-grained, discontinuous and vary in thickness from 0.5 to 2 m and up to 1.4 km in length. These dykes cut both the metamorphosed sandstones and porphyritic biotite granite. The trends of these dykes are concordant with the main structural trends affected in the study area, so that they run in NW-SE, NNE-

SSW and N-S.

Particle track analyses

Some samples from the different mineralized parts of metamorphosed sedimentary rocks were submitted to α -track analyses as a mean of micromapping the radioelement distribution.



Figure 3. Field photographs: (a) lamprophyre dyke runs NW-SE and cuts metamorphosed sandstone; (b) Lens-like of metamorphosed sandstone inliers within granitic rocks; (c) Alteration zone of metamorphosed sandstone; (d) relics of bedding in quartzite showing disturbed direction; (e) Left lateral movements of strike slip runs NNE-SSW; (f) hematitizations (Fe) and manganese oxides (Mn) along shear zones.

the rock with remarkable epidotization and sericitization of plagioclase. The biotite and muscovitic grains are enriched in uranium mineralization along their outer boundaries and their

cleavage planes (Figure 5a to d). It appears that biotite acts as reductant, precipitating the uranium. Chlorites, sericitized plagioclase and highly fractured quartz grains also contain uranium

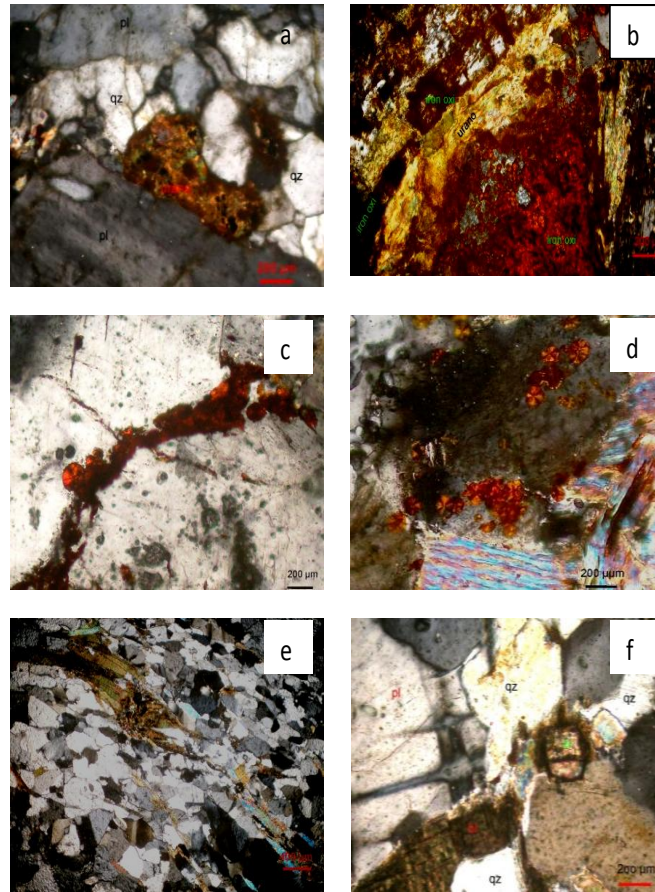


Figure 4. Photomicrographs showing: (a) Uranophane crystal (urano.) interstitial between quartz and plagioclase; (b) uranophane associating iron oxides (iron oxi.); (c) autonite occurs as filling fracture in quartz; (d) autonite on the surface of crystals; (e) metamict zircon (zr).

mineralization (Figure 5e and f). Most of the rocks forming minerals are stained with iron oxides which occasionally adsorb uranium causing intense uranium mineralization (Figure 5g and h).

Radionuclides investigation

The radioelement measurements of the studied metamorphosed sandstone samples are shown in Table 1. Metasediments show wide variation in their U, Th, Ra (eU) and K% contents. They show variation of U from 3 to 24 ppm, with an average of 10 ppm and Th content between 2 and 47 ppm, with 14.57 ppm as an average. Ra (eU) vary between 2 and 18 ppm with an average of 8.07 ppm (Table 1).

When the data of the studied metasediments are compared with the averages of arenaceous and argillaceous sediments (Table 1) reported by IAEA (1979) and Boyle (1982), it is clear that Wadi Sikait samples have higher contents of uranium and thorium than the arenaceous sediments and also the average of greywacke reported by Killeen (1979). Average of uranium contents are higher than argillaceous sediments while average of thorium values fall within the range of argillaceous sediments. Th/U ratio average (1.59 ppm) is lower than average of arenaceous and argillaceous

sediments. It is worth to mention that the relatively high values of U and Th in the studied metasediments are mainly related to the presence of radioactive accessory minerals such as metamict zircon, monazite, xenotime, allanite, uranophane and autonite observed in their thin sections.

The U-contents and Th/U ratios in sedimentary rocks are generally used to deduce the conditions under which the highly anomalous mineralized or uraniferous types were formed (Adams and Weaver, 1958). However, three types of sediments are differentiated according to their Th/U ratios:

- i) The first type includes sediments of Th/U ratio value ranging between 0.012 to 0.81. These sediments are developed under conditions where uranium was removed from its source and fixed in the sediments with continuous recharge.
- ii) The second type of sediments has Th/U ratio value ranging between 1.47 to 1.49. They are characterized by their relatively high Th-content due to slightly more scavenging of U-content because of continuous leaching and recharging.
- iii) The third type of sediments exhibits Th/U ratio value ranging between 1.49 and 5.47. These sediments reflect the poor weathering and rapid deposition of rock detritus. Therefore, the detrital radioactive minerals like xenotime, samarskite, thorite and

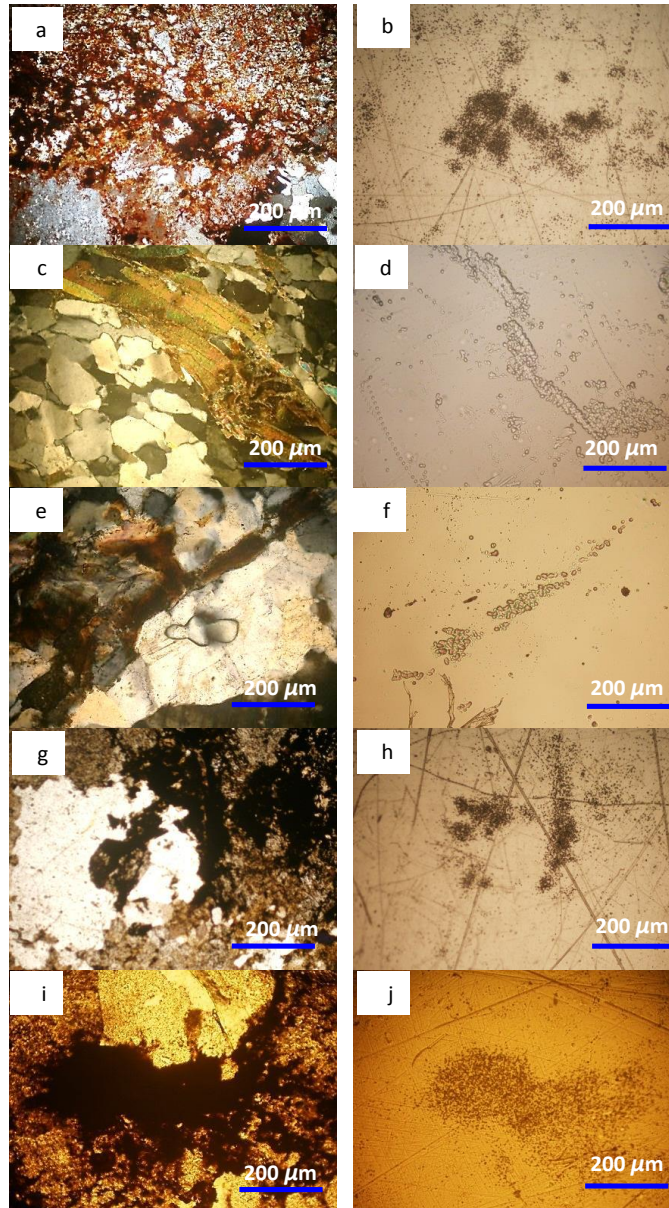


Figure 5. (a) Radioactive-mineralization along grain boundaries and in crystal lattice of allanite, zircon and monazite; (b) and its corresponding dense alpha track image showing radioactive minerals; (c, d, e and f) biotite and muscovite grains are enriched in uranium mineralization along their outer boundaries and their cleavage planes and its corresponding dense alpha track image showing radioactive minerals; (g and h) chlorites, sericitized plagioclase and highly fractured quartz grains also contain uranium mineralization; (i and j) iron oxides stained with uranium causing intense uranium mineralization and its corresponding dense alpha track image showing dense and disseminated radioactive minerals.

euxenite usually dominate them.

The obtained data indicates that the eTh/eU ratio values of the metamorphosed sandstone are low to medium values, ranging between 0.11 to 4.33, with 1.75 as an average (Table 1 and Figure 6). This means that they are related to more than one group,

suggesting different conditions prevailing during uranium deposition. A high uranium content of the metamorphosed sandstone is attributed to presence of radioactive minerals like uranophane and autonite (Figure 4a and b) in addition to accessory minerals like allanite, zircon and monazite (Figure 5c to f).

Table 1. U, Th, Ra (eU) and K contents and some isotopic ratios.

Sample No.	Cup No.	Sample code	eU (ppm)	e Th (ppm)	Ra (eU) (ppm)	K%	Th/U	P-factor U/Ra	U _c	D-factor
1	45	N-S Sh 1-1 (1)	7	11	4	3.86	1.57	1.75	-	-
2	45	N-S Sh 1-1-(2)	4	9	5	3.35	2.25	0.8	-	-
3	42	N-S Sh1-1 (1)1	5	7	4	2.79	1.4	1.25	-	-
4	43	N-S Sh1-1 (1) 2	8.58	16.69	8.01	2.7	1.95	1.06	-	-
5	42	N-S Sh1-1 (2) 2	5	2	5	1.53	0.4	1	-	-
6	43	N-S Sh1-1 (3) 1	8	10	4	3.45	3.33	0.75	-	-
7	43	N-S Sh1-1 (3) 2	3	13	5	4.64	4.33	0.6	-	-
8	25	N-S Sh 1-6 1	29.38	90.84	56.22	5.67	3.09	0.52	35	1.19
9	45	N-S Sh 1-7 2	7	5	4	3.28	0.71	1.75	-	-
10	32	N-S Sh 2-1 1	10.85	20.04	8.48	3.63	1.85	1.28	-	-
11	44	N-S Sh 2-1 2	8.32	9.98	9.78	2.36	1.2	0.85	-	-
12	50	N-S Sh 3-1 (1)	10.51	20.13	9.97	3.71	1.92	1.05	-	-
13	50	N-S Sh 3-1 (2)	19.63	38.89	17.27	4.04	1.98	1.14	60	3.06
14	51	N-S Sh 3-2 (1)	3	2	0	0	1.33	1	-	-
15	51	N-S Sh 3-2 (2)	7.21	16.86	7.16	2.94	2.34	1.01	-	-
16	50	N-S Sh 3-3 (1)	20	45	12	0.36	2.25	1.09	40	2
17	53	N-S Sh 3-3 (2)	9.2	21.6	8.75	2.41	2.35	1.05	-	-
18	54	N-S Sh 2-3 B (1)	18.9	51.54	11.75	0.76	2.73	1.61	-	-
19	54	N-S Sh 2-3 B (2)	20	40.55	14.25	1.31	2.03	1.4	-	-
20	49	N-S Sh 4-1 (1)	6	15	7	2.78	1.96	2.4	-	-
21	59	N-S Sh 4-1 (2)	41.97	5.44	48.3	2.22	0.13	0.87	-	-
22	67	N-S Sh 5-1 a (1)	16	17	9	3.11	1.06	1.78	100	6.25
23	68	N-S Sh 5-1 a (2)	10	15	10	2.77	1.15	1.3	-	-
24	69	N-S Sh 5-2 (1)	17.14	29.91	15.23	5.4	1.75	1.13	50	-
25	69	N-S Sh 5-2 (2)	24.85	2.84	16.21	2.33	0.11	1.53	-	-
26	32	NNE-SSW Sh 2-1 2	5	21	8	4.16	4.2	0.63	-	-
27	35	NNE-SSW Sh 2-2 1	7	2	5	5.11	0.29	1.4	-	-
28	35	NNE-SSW Sh 2-2 2	7	2	5	4.52	0.29	1.4	-	-
29	33	NNE-SSW Sh 2-3 1	17	16	16	0.35	0.94	1.06	20	-
30	33	NNE-SSW Sh 2-3 2	8.41	12.6	9.02	3.1	1.5	0.93	-	-
31	63	NNE-SSW End of zone2 (1) at 63	15	22	7	2.03	1.47	2.14	-	-
32	63	NNE-SSW End of zone2 (2) at 63	7	13	6	3.93	1.86	1.17	-	-
33	37	NW-SE Sh 3-1 1	15	19	8	4.26	1.27	1.88	-	-
34	36	NW-SE Sh 3-1 2	9	19	9	4.46	2.11	1	-	-
35	38	NW-SE Sh 3-2 1	12	21	8	4.14	1.75	1.5	-	-

Table 1. Contd.

36	38	NW-SE Sh 3-2 2	10	18	9	4.14	1.8	1.11	-	-
37	39	NW-SE Sh 3-2 R 1	10	17	7	4.09	1.7	1.43	-	-
38	39	NW-SE Sh 3-2 R 2	12	16	7	4.93	1.33	1.71	-	-
39	40	NW-SE Sh 3-3 1	9	22	11	3.2	2.44	0.82	-	-
40	40	NW-SE Sh 3-3 2	16	23	10	3.39	1.44	1.6	-	-
Average			12	19	10.64	3.18	1.75	1.24	50.83	2.77
Minimum			3	2	0	0	0.11	0.52	20	1.18
Maximum			41.97	90.84	56.22	5.67	4.33	2.4	100	6.25
Arenaceous sediments (IAEA, 1979; Boyl, 1982)			1	3	-	1.4	3	-	-	-
Argillaceous sediments (IAEA, 1979; Boyl, 1982)			4	16	-	2.7	4	-	-	-
Average of greywacke (Killen, 1979)			1.5	5	-	-	-	-	-	-

Other U-bearing minerals are also recorded as biotite, muscovite, iron oxides and clays (Figure 5i and j).

Radioactive equilibrium

Both U and Ra are mobile from a chemical point of view. At this step we just can observe that disequilibrium exists, but we do not know if it is due to a U enrichment or a Ra impoverishment. According to Reeves and Brooks (1978), uranium (U^{238} series) attains the equilibrium state in nearly 1.5 M.a. Cathelineau and Holliger (1987) stated that uranium mineralization is affected by different processes. Leaching, mobility and redistribution of uranium are affected by hydrothermal solutions and/or supergene fluids which cause disequilibrium in the radioactive decay series in the U-bearing rocks. The radioactive equilibrium of the studied metasediment can be determined by the calculation of equilibrium factor (P) which is the ratio of radiometric uranium contents (eU) to the radium content Ra(eU); $P_{\text{factor}} = eU/Ra(eU)$ (Husseini, 1978; El-Galy, 1998; Surour et al., 2001; Raslan and El-Feky, 2012; Nadaa and Aly, 2014).

The average of P-factor of the studied metasediment is 1.24 (Table 1), indicating disequilibrium in U-decay is due to addition of uranium to these rocks. The second method for the study of equilibrium is carried out by using the data

of chemically analyzed uranium (U_c) and radiometrically determined uranium (U_r). Ratio between chemically and radiometrically measured uranium is known as the D-factor = U_c/U_r (Hansink, 1976). The use of D-factor in the determination of equilibrium state of the studied rocks reveals that nearly all the studied rocks have chemically analyzed uranium greater than the radiometrically determined uranium reflecting a disequilibrium state characterized by addition of uranium.

Evidences of recent uranium mineralization

Radiometric techniques (gamma-ray spectrometry, particle track analyses), in addition to chemical analysis were employed to determine the abundance and distribution of U-series nuclides, the extent of secular equilibrium within the U decay series. Young deposits are of apparent economic interest in view of their common occurrence, amenability to *in situ* leaching and lack of radioactive components. The uranium tends to be loosely held in recent uranium deposits and as it is too recently deposited to have built up radioactive daughter products; concentrations are seldom detectable by scintillometer. Though there was detection of surficial uranium mineralizations in the studied rocks by microscopic and α -track investigations and as a result of their young ages, the

studied deposits have not yet reached radioactive secular equilibrium and therefore, yielded very little gamma activity (Table 1). Also, there is an apparent difference between radiometrically and chemically measured uranium (Table 1), suggesting recent U-deposition. The immobility of Th is supported by whole-rock Th contents which do not vary significantly with U content (Figure 6). Activity ratios (AR) of $^{230}\text{Th}/^{234}\text{U}$ in rocks, which range from 0.43 to 1.3, demonstrate recent U accumulation and leaching (Hassan et al., 2014), suggesting recent uranium mineralization.

Radon exhalation rates from the studied rocks were measured using "Sealed Can technique" and indicated the presence of subsurface and surface uranium anomaly which confirms the previous results (Hassan et al., 2014).

Conclusion

The metamorphosed sandstones occur in two locations in Wadi Sikait (Sikait-1 and Sikait-2). The main outcrops are ophiolitic mélange, metamorphosed sandstones, biotite granites and post-granite dykes (lamprophyres) and veins (fluorite and quartz). Radiometrically measured uranium contents reach up to 41.97 ppm while

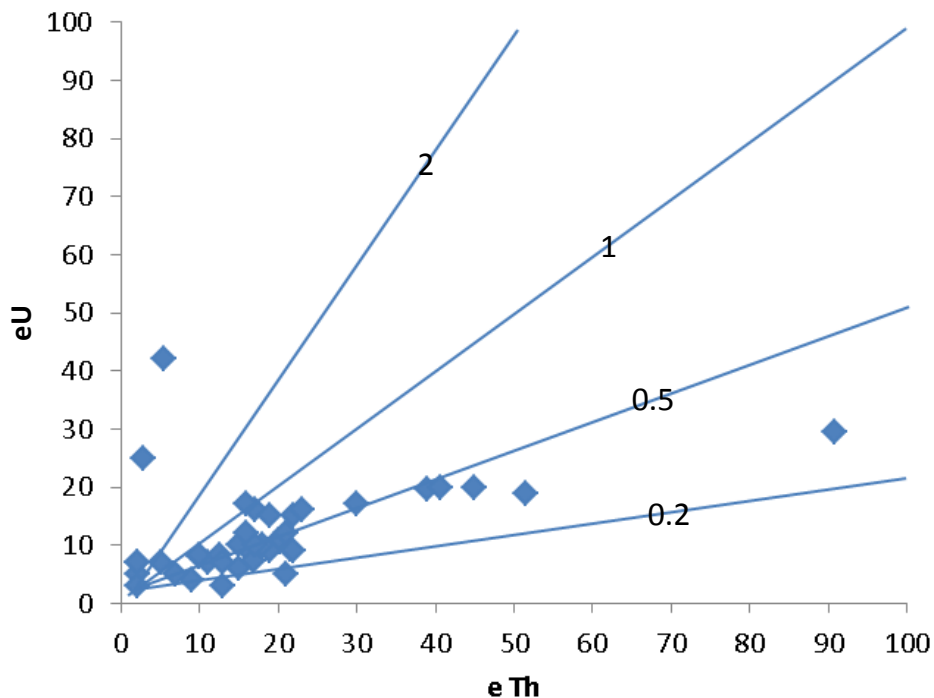


Figure 6. eU-eTh diagram of the studied metamorphosed sandstone.

chemically recorded measurements reach 100 ppm. High uranium contents may be attributed to the presence of uranophane, autonite, zircon, monazite, allanite, iron oxides and clay minerals.

Radiometric techniques and chemical analysis were employed to determine the abundance and distribution of U-series nuclides, the extent of secular equilibrium within the U decay series. Though in the detection of surficial uranium mineralizations in the studied rocks by microscopic and α -track investigations and as a result of their young ages, the studied deposits have not yet reached radioactive secular equilibrium and therefore, yield very little gamma activity. Also, there is an apparent difference between radiometrically and chemically measured uranium, suggesting recent U-deposition. The immobility of Th is supported by whole-rock Th contents which do not vary significantly with U content. Activity ratios (AR) of $^{230}\text{Th}/^{234}\text{U}$ in rocks, which range from 0.43 to 1.3 demonstrate recent U accumulation and leaching, suggesting recent uranium mineralization. Radon exhalation rates from the studied rocks were measured using "Sealed Can technique" and indicated the presence of subsurface and surface uranium anomaly which confirms the previous results.

Conflict of Interest

The author(s) have not declared any conflict of interests.

REFERENCES

- Adams JAS, Weaver CE (1958). Thorium to uranium ratios as indicator for sedimentary processes; An example of geochemical facies. *Am. Assoc. Petrol. Geol.* 42:397-430.
- Assaf HS, Ibrahim ME, Zalata AA, El-Metwally A, Asaleh GM (2000). Polyphase folding in Nugrus- Sikeit area, south Eastern Desert, Egypt. *JKAW: Earth Sci.* 12:1-16.
- Boyle RW (1982). *Geochemical prospecting for thorium and uranium deposits.* Elsevier Publ. Co., Amsterdam. P498.
- Cathelineau M, Holliger P (1987). Polyphase metallogenesis of hydrothermal uranium veins from the southern amonicon massif, France. *Proc. Int. Mtg Nancy.* Pp.212-217.
- El-Ramly MF, Greiling RO, Kroner A, Rashwan AA (1984). On the tectonic evolution of the Wadi Hafafit area and environs EDE, *Bulletin Faculty Earth Science King Abdulaziz University* 6:113-126.
- El-Galy MM (1998). *Geology, radioactivity, geochemistry and tectonic setting of selected granitic rocks, West Gulf of Aqaba, Sinai, Egypt,* Ph.D Thesis, Tanta Univ., Egypt. P.324.
- Florou H, Kritidis P (1992). Gamma radiation measurements and dose rate in the coastal areas of a volcanic island, Aegean Sea, Greece. *radiat. Port. Dosim.* 45(1/4):277-279.
- Greiling RO, Abdeen MM, Dardir AA, El Akhal H, El Ramly MF, Kamal El Din GM, Osman A F, Rashwan AA, Rice AHN, Sadek MF (1994). A structural synthesis of the Proterozoic Arabian-Nubian Shield in Egypt. *Geol. Rundsch.* 83:484-501.
- Greiling RO, Kroner A, El-Ramly MF, Rashwan AA (1988). Structural relationships between the southern and the central parts of the Eastern Desert of Egypt: details of a fold and thrust belt. In: El-Gaby S, Greiling RO (Eds.). *The Pan-African Belt of NE Africa and the Adjacent Areas-Tectonic Evolution and Economic Aspects of a Late Proterozoic Orogen.* Frieder Vieweg and Sohn, Braunschweig/Wiesbaden, Germany, Pp.121-145.
- Hansink JD (1976). Equilibrium analysis of sandstone rollfront uranium deposits. *Proceeding of International Symposium on Exploration of uranium ore deposits.* IAEA, Vienna. Pp.683-693.
- Harraz HZ, EL-Sharkawy MF (2001). Origin of tourmaline in the

- metamorphosed Sikait pelitic belt, south Eastern Desert. Egypt J. Afr. Earth Sci. 33(2):391-416.
- Hashad AH, El Reedy MWM (1979) Geochronology of the anorogenic alkalic rocks, South Eastern Desert. Egypt J. Ann. Geol. Surv. Egypt. 9:81-101.
- Hassan MA, Hashad AH (1990). Precambrian of Egypt. In: Said R. (ed.). The geology of Egypt, Balkema, Rotterdam, Pp.201-245.
- Hassan SF, Abu Elatta SA, El-Farrash AH, El-Feky MG, Refaat M (2014). U-series radionuclides disequilibria as indication of recent U-mobilization in mineralized Low grade metamorphosed sandstone-type uranium deposit, Wadi Sikait, South Eastern Desert, Egypt, in press.
- Hegazy HM (1984). Geology of Wadi El Gemal area, Eastern Desert, Egypt. Ph. D. Thesis, Assiut Univ., Egypt. P. 271.
- Hussein HA (1978). Lecture course in nuclear geology. P. 101.
- IAEA (1979). International Atomic Energy Agency. "Gamma-Ray Survey in Uranium Exploration". IAEA Technical Report Series, No. 186, Vienna, Austria, P.90.
- Ibrahim ME, Abdel-Wahed AA, Oraby F, Abu El-Hassan El Galy MM, Watanabe K (2007). factors controlling mineralization in lamprophyre dyke, Abu Rushied area, Eastern Desert, Egypt. 5 th International Conf. on the geology of Africa Assiut – Egypt. 1:79-92.
- Ibrahim ME, Amer TE, Saleh GM (1999). New occurrence of some nuclear materials and gold mineralization at Wadi Sikait area , south Eastern Deser, Egypt .First seminar on Nuclear Raw Materials and their technology,Cairo,Egypt. Pp.271-284.
- Ibrahim ME, Saleh GM, Ibrahim WS (2010). Low grade metamorphosed sandstone-type uranium deposit, Wadi Sikait, South Eastern Desert. Egypt. J. Geol. Min. Res. 2(6):129-141.
- Killeen PG (1979). Gamma ray spectrometric methods in uranium exploration—application and interpretation; *in* Geophysics and Geochemistry in the Search for Metallic Ores; Hood, P.J., ed., Geol. Surv. Can. Econ. Geol. Report 31:163-229.
- Matoline M (1991). A report to the government of the Arab Republic of Egypt. "Construction and use of spectrometric calibration pads", Egypt. Laboratory gamma-ray spectrometry.
- Mohamed FH, Hassanen MA (1997). Geochemistry and petrogenesis of Sikait leucogranite, Egypt: an example of S-type granite in a metapelitic sequence. J. Geol. Rundsch. 86:81-92.
- Nadaa A, Aly HAS (2014). The Effect of Uranium Migration on Radionuclide Distributions for Soil Samples at the El-Gor Area, Sinai, Egypt. Appl. Radiat. Isotopes. 84:79-86.
- Omar SA (1995). Geology and geochemical features of the radioactive occurrences of Um-Anab granitic masses, Eastern Desert, Egypt, M.Sc. Thesis, Cairo University. P.195.
- Raslan MF, El-Fekyy MG (2012). Radioactivity and mineralogy of the altered granites of the Wadi Ghadir shear zone, South Eastern Desert, Egypt. Chin. J. Geochem. 31(1):30-40.
- Reeves RD, Brooks RR (1978). Trace element analyses of geological materials. John Wiley & sons Inc., New York, P.421.
- Saleh GM (1998). The potentiality of uranium occurrences in Wadi-Nugrus area, South Eastern Desert: Unpubl. Ph.D. thesis, Faculty of Science, Mansoura University P.171.
- Saleh GM Abdallah SA, Abbas AA, Dawood NA, Rashed MA (2012). Uranium mineralizations of Wadi Sikait mylonites, Southeastern Desert. Egypt J. Geol. Min. Res. 3(5):86-104.
- Stern RJ, Hedge CE (1985). Geochronologic and isotopic constraints of Late Preeambrian crustal evolution in the Eastern Desert of Egypt. Am. J. Sci. 285:97-127.
- Surour AA, El-Bayoumi RM, Attawiya MY, El-Feky MG (2001). Geochemistry of wall rock alterations and radioactive mineralization in the vicinity of Hangaliya auriferous shear zone, Eastern Desert, Egypt. Egypt. J. Geol. 45(1):187-212.
- UNSCEAR (1993). Sources and effects of ionising radiation. Report to general assembly, with scientific annexes, United Nations, New York.